

Solvent Dependence of Electronic Relaxation in All-trans Retinal Studied by One- and Two-Photon Induced Transient Absorption

Erica J. Larson,[†] Sarah J. Pyszczynski, and Carey K. Johnson*

Department of Chemistry, University of Kansas, Lawrence, Kansas 66045

Received: April 24, 2001; In Final Form: June 25, 2001

One- and two-photon excited ultrafast transient absorption measurements are reported for all-trans retinal in polar, nonpolar, and hydrogen-bonding solvents. A comparison of the response following one- and two-photon excitation allows assignment of the observed decays to the ${}^1B_u^+$ -like and ${}^1A_g^-$ -like excited states. In the polar, hydrogen-bonding solvent ethanol, the transient absorption changes following one-photon excitation are dominated by a 2-ps response observed both in the decay of transient absorption and in the decay of stimulated emission observed in the region from 600 to 750 nm. Because of the strong stimulated emission gain, this response can be assigned to decay of the strongly optically allowed “ ${}^1B_u^+$ ” state. With two-photon excitation of all-trans retinal in ethanol, a 200–300 fs decay component appears as well and is assigned to decay of the “ ${}^1A_g^-$ ” state, which has a large two-photon cross section. In contrast, for all-trans retinal in hexane, both 200–300 fs and 2-ps decay components are observed following one-photon excitation, and no stimulated emission is detected. A comparison of one- and two-photon induced transient absorption leads to an assignment of the decay events. The ultrafast responses of all-trans retinal in the polar, aprotic solvents acetonitrile and propionitrile are found to be similar to the response in ethanol, indicating that protic solvents act through solvent polarity rather than a specific effect of hydrogen bonding. The effect of hydrogen bonding was studied further for all-trans retinal in mixed solvents with varying concentrations of trifluoroacetic acid, a strong hydrogen-bond donor, in hexane. As the ratio of trifluoroacetic acid to retinal increased from 1:5 to 10:1, the ultrafast response changed smoothly from “hexane-like” to “ethanol-like”, with an increasingly strong stimulated emission component having a 2-ps decay, in agreement with the increased fluorescence quantum yield observed in polar and hydrogen-bonding solvents. A model is proposed incorporating two populations of retinal having different electronic relaxation pathways to explain the solvent-dependent photophysics of all-trans retinal.

Introduction

The photophysics of retinal has been a subject of long-standing interest, both because of its role in photoactive proteins such as bacteriorhodopsin and because of its fundamental photophysics.^{1–3} Because several relaxation channels, including internal conversion (IC), intersystem crossing (ISC), vibrational relaxation, and photoisomerization, compete over the time scale from tens of femtoseconds to tens of picoseconds, the fate of electronic excitation is decided within a few picoseconds or less. Recent results from several laboratories^{4–11} have begun to unravel the ultrafast events in relaxation of retinals. However, a consensus has not yet been reached on the identity of the relaxation steps of all-trans retinal. In our laboratory, we have studied ultrafast relaxation of retinal in both polar and nonpolar solvents, and we have compared the relaxation processes following transient absorption induced by one-photon excitation (OPE) and two-photon excitation (TPE).⁶ Differences were observed in the initial ultrafast relaxation events as a result of different selection rules for OPE and TPE, which launch the excited-state relaxation from different excited states. These differences between one- and two-photon excited transient absorption have allowed us to sort out contributions from different excited states to the observed transient signals.⁶

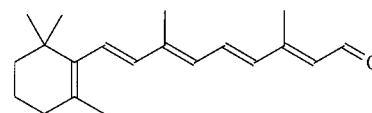


Figure 1. Structure of all-trans retinal.

The ultrafast response in all-trans retinal (ATR, Figure 1) involves three excited singlet states that lie close together in energy: two $\pi\pi^*$ states and one $n\pi^*$ state. The $\pi\pi^*$ states in retinal are labeled by the C_{2h} group symmetry labels “ ${}^1B_u^+$ ” and “ ${}^1A_g^-$ ”, which recognize that the electronic structures of these states correlate with those of the corresponding all-trans polyene. (The quotation marks indicate that the C_{2h} symmetry labels, which denote the character of the excited state, are only approximate for retinal.) A central issue in understanding the photophysics of retinal has been the ordering of the singlet excited electronic states of retinal. Of the three close-lying excited singlet states (${}^1n\pi^*$, “ ${}^1A_g^-$ ”, and “ ${}^1B_u^+$ ”), the optically allowed “ ${}^1B_u^+$ ” state has the highest energy.¹² One-photon absorption therefore excites predominantly (but not exclusively¹²) the S_3 (“ ${}^1B_u^+$ ”) state. The “ ${}^1A_g^-$ ” state was found to lie some 2400 cm^{-1} below the “ ${}^1B_u^+$ ” state.¹² However, the relative ordering of the two lower-energy excited states, “ ${}^1A_g^-$ ” and ${}^1n\pi^*$, has been more difficult to determine. In nonpolar solvents, the evidence for a lowest-lying singlet $n\pi^*$ state includes (1) efficient ISC to a ${}^3A_g^-$ (T_1) state, implicating ISC from an ${}^1n\pi^*$ S_1 state to the ${}^3\pi\pi^*$ - T_1 state;¹³ and (2) the low

* To whom correspondence should be addressed. E-mail: ckjohnson@ku.edu.

[†] Current address: Chemical Sciences and Technology Division, Los Alamos National Laboratory, MS M888, Los Alamos, NM 87545.

fluorescence quantum yield of ATR in nonpolar solvents, which was taken as evidence for the $n\pi^*$ character of S_1 .¹⁴ The higher fluorescence quantum yield and lower ISC yield of ATR in polar solvents were correspondingly thought to indicate a solvent-induced inversion of the ordering of the $n\pi^*$ and ${}^1A_g^-$ states.¹⁵ However, recent results have called this conclusion into question.¹⁰

In a previous study of ATR in ethanol excited at 400 nm, we detected two ultrafast relaxation events.^{6,10} A 2-ps decay was observed both in transient absorption and in stimulated emission. The observation of stimulated-emission gain shows that the state undergoing relaxation is strongly optically allowed. Accordingly, this state can be identified as the ${}^1B_u^+$ state. This assignment is supported by semiempirical calculations and experimental measurements of the ${}^1B_u^+$ oscillator strength for ATR in the polar solvent EPA.¹² In contrast to the transients induced by one-photon excitation, two-photon excitation at 800 nm revealed a faster decay of 300 fs.⁶ Furthermore, no stimulated emission was observed following TPE. Because TPE excites predominantly the ${}^1A_g^-$ state,¹² we assigned the 300-fs component to relaxation of the ${}^1A_g^-$ state. Transient absorption measurements were also reported recently for ATR in 1-butanol and in 1-butanol/hexane mixed solvents by Yamaguchi and Hamaguchi.¹¹ These workers also observed stimulated emission gain with a decay time of 1.9 ps. However, they assigned this component to relaxation of the ${}^1A_g^-$ state, and they assigned a 700-fs decay component to the ${}^1B_u^+$ state. This assignment is contingent upon an assumption that the oscillator strength of the ${}^1A_g^-$ state is larger than that of the ${}^1B_u^+$ state. This assumption is not in agreement with previous spectroscopic measurements and semiempirical calculations.¹²

Recent ultrafast transient absorption measurements have occasioned a reconsideration of the solvent dependence of the excited-state level ordering.^{10,11} The temperature dependence of the decay of the ${}^1B_u^+$ state was followed down to 80 K.¹⁰ From the decay time of the ${}^1B_u^+$ state and its estimated radiative lifetime, the fluorescence quantum yield was calculated.¹⁰ The values, both at room temperature and at 80 K, were found to agree closely with the corresponding measured fluorescence quantum yields, showing that emission from the ${}^1B_u^+$ state accounts for the observed fluorescence yield, and that a weakly fluorescent lowest-lying ${}^1A_g^-$ state is not required to explain the observed fluorescence quantum yield, as had previously been thought. Second, we found that the ISC time in a polar solvent (ethanol) is as fast as the ISC time in the nonpolar solvent hexane,⁶ suggesting a similar $S_1(n\pi^*) \rightarrow T_1({}^3\pi\pi^*)$ mechanism of ISC in both solvents. Although we had previously accepted the prevailing idea that the level ordering is solvent dependent with a lowest lying ${}^1n\pi^*$ state in nonpolar solvents and a lowest lying ${}^1A_g^-$ state in polar solvents,⁶ these results suggested that the lowest lying excited singlet state retains $n\pi^*$ character, even in hydrogen-bonding solvents.¹⁰

In the present paper, we address the question of whether there exists a specific effect of hydrogen bonding, or whether the differences that have been observed between electronic relaxation of ATR in alkanes and alcohols are a result of solvent polarity. We compare the ultrafast relaxation events for ATR in the nonpolar solvent hexane, the hydrogen-bonding solvent ethanol, and in the aprotic polar solvents acetonitrile and propionitrile. We also report experiments for ATR in binary mixed solvents consisting of hexane with a small mole fraction of a hydrogen-bonding cosolvent (trifluoroacetic acid) to investigate the possibility of specific hydrogen-bonding effects. We find that as the amount of trifluoroacetic acid is increased,

the ultrafast response changes smoothly from a response characteristic of the nonpolar solvent hexane to one characteristic of the polar solvents ethanol and acetonitrile, with an increasingly strong stimulated emission component having a 2-ps decay. No evidence is found that a new decay channel involving proton transfer, for example, is introduced by hydrogen bonding.

Methods

Steady-state absorption spectra were measured with a Cary 50 spectrophotometer. Transient absorption measurements were carried out with a femtosecond Ti-sapphire laser system. Further details are available in a previous publication.⁶ ATR was excited at either 400 (for one-photon excitation) or 800 nm (for two-photon excitation) with pump pulses of 150 fs at a 1-kHz repetition rate. The pump power was typically 10–20 mW at 400 nm or 50–200 mW at 800 nm, focused to a spot size of ~ 1 mm (larger for two-photon excitation). Optical densities at 400 nm were around 1. Probe pulses were selected from a continuum with an interference filter centered at the desired wavelength. Pump and probe pulse polarizations were set to the magic angle to eliminate orientational effects. Transient absorption measurements were obtained in the small-signal limit as

$$\Delta A = -\left(\frac{I - I_0}{I_0}\right)_{\text{pump}} + \left(\frac{I - I_0}{I_0}\right)_{\text{no pump}} \quad (1)$$

where I is the signal intensity, and I_0 is the reference intensity set equal to I in the absence of a pump pulses. The second term, which is nominally zero, was included to correct for any drift between probe and reference channels. Samples were flowed through a flow cell with path length of 1 mm for one-photon excitation and 2 mm for two-photon excitation.

Results and Discussion

One-Photon and Two-Photon Induced Transient Absorption of All-trans Retinal. Transient absorption scans of ATR in hexane and ethanol excited at 400 nm are shown in Figure 2. (Several of these transient absorption scans were reported previously⁶ and are included here for completeness.) Decay times and amplitudes obtained by fitting to these decays are tabulated in Table 1. Clear differences are observable between the relaxation components in the two solvents. In hexane, a fast decay of 300 fs or less dominates the response at longer wavelengths. In contrast, in ethanol over the first 10 ps, we found a single time constant of 1.8–2.1 ps at all wavelengths probed. This ~ 2 -ps response also appears in stimulated emission at 650–750 nm in ethanol. The initial rise in the transient absorption in some scans (for example at 700–750 nm) is a power-dependent artifact. Similar artifacts have been identified previously¹⁶ and attributed to phase modulation of the probe pulse by the pump pulse.

To identify the contributions of the ${}^1B_u^+$ and ${}^1A_g^-$ states to the transient signals, we also carried out two-photon induced transient absorption measurements. Results are shown in Figure 3, and fitted decay times and amplitudes are given in Table 2. (Some of these results were also reported previously.⁶) Because of the higher pulse intensities used for two-photon excitation, we checked for nonresonant, nonlinear contributions induced by the 800-nm pump beam by comparing the response with and without ATR. Such contributions were absent at probe wavelengths of 600 nm or shorter but were observed at probe wavelengths of 650 nm or longer. The observed response at shorter wavelengths can therefore be attributed to resonant processes.

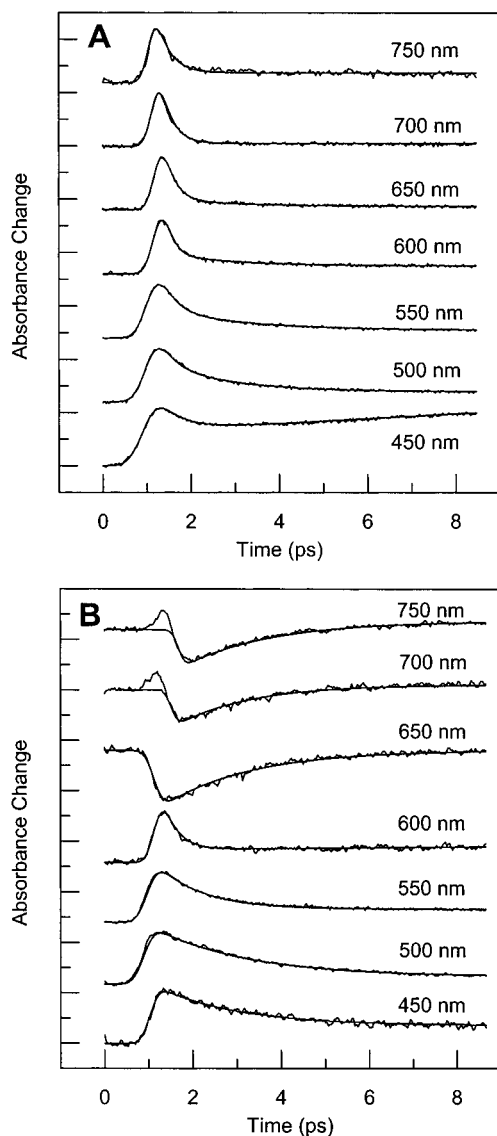


Figure 2. One-photon induced transient absorption scans of ATR in (A) hexane and (B) ethanol. Excitation was at 400 nm. The smooth solid lines show fits to the data. Scans have been normalized.

The two-photon induced transient signals differ in several important and revealing respects from the corresponding one-photon induced responses in Figure 2. For ATR in ethanol, a fast subpicosecond component becomes apparent in the TPE induced transient absorption, while the 1–2 ps component that is so prominent in the one-photon excited spectra is reduced in amplitude. Notably, the stimulated emission gain is absent with TPE. For ATR in hexane, the 1–2 ps component is discernible only at 500 and 550 nm in the TPE induced transient absorption spectra, in contrast to the OPE induced transient absorption spectra, where the 1–2 ps component was found throughout the region from 450 to 650 nm. Thus, for ATR in both hexane and in ethanol, the fast response (300 fs) is more dominant with TPE, while the slower (1–2 ps) component is favored by OPE.

We have constructed transient absorption spectra from single-wavelength measurements at 50-nm intervals from 450 to 750 nm. Spectra for ATR in hexane with one- and two-photon excitation are shown in Figure 4. The one-photon spectra of ATR in hexane show a strong initial transient absorbance peaking at 550 nm that decays and narrows within the first picosecond. This absorption decays further in a few picoseconds as the $T_1 \rightarrow T_n$ absorbance begins to grow in at 450 nm. These

TABLE 1: Fitting Parameters for One-Photon Transient Absorption Data of All-trans Retinal in Hexane and Ethanol^a

λ probe (nm)	τ_1 (fs)	amp.	τ_2 (ps)	amp.	τ_3 (ps)	amp.
all-trans retinal in hexane						
380	340	-0.81	3.0	0.06	45 ± 15	0.13
450	300 (fixed)	0.45	1.8 ± 0.2	0.15	29 ± 6	-0.4
500	300 (fixed)	0.72	1.8 ± 0.3	0.23	31 ± 11	-0.05
550	300 (fixed)	0.75	1.9 ± 0.5	0.19	24 ± 1	0.06
600	250 ± 70	0.84	1.3 ± 0.5	0.12	29 ± 16	0.04
650	260 ± 160	0.84	3.2 ± 2.7	0.11	21	0.05
700	240 ± 14	0.97			28	0.03
750	190 ± 160	1.0				
all-trans retinal in ethanol						
380	0.60 ± 0.30	-0.50	2.2 ± 2.0	0.29	47 ± 8	0.21
450			1.9 ± 0.1	0.91	25 ± 7	-0.09
500			2.1	0.91	32 ± 7	-0.09
550			1.2 ± 0.2	0.96	21 ± 7	-0.04
600			0.21 ± 0.11	0.93	25	-0.07
650			1.8 ± 0.2	1.0		
700			1.8 ± 0.1	1.0		
750			1.9 ± 0.1	1.0		

^a Errors are based on a calculation of the standard deviation of a series of measurements, except for 380 nm in which only a single measurement was obtained. The amplitude columns give the relative amplitudes of the decay components, normalized so that the sum of the amplitudes at a particular probe wavelength is 1.

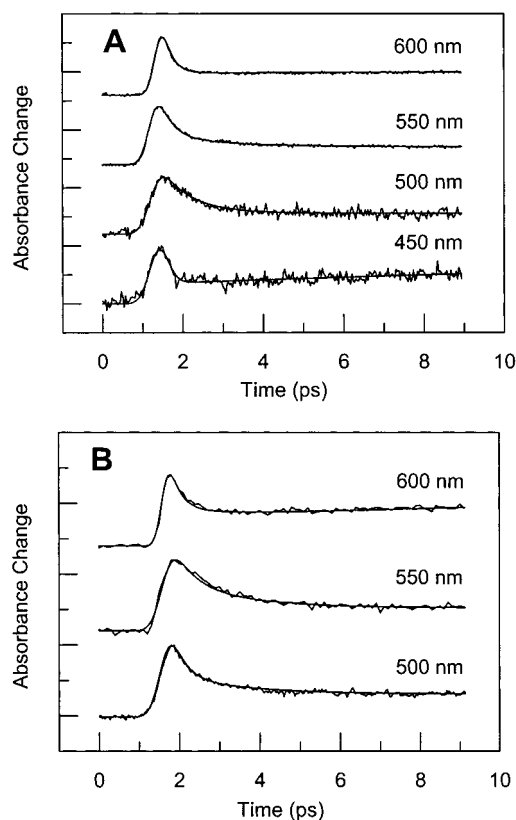


Figure 3. Two-photon induced transient absorption scans of ATR in (A) hexane and (B) ethanol. Excitation was at 800 nm. The smooth solid lines show fits to the data. Scans have been normalized.

features corroborate our previous single-wavelength time scans.⁶ In the two-photon induced transient absorption spectra of ATR in hexane, the decay of the transient absorption is more rapid overall, consistent with the increased weight of the fast (200–300 fs) decay component. The comparison of OPE and TPE induced transient absorption spectra in hexane over the first few picoseconds (Figure 4) shows that ATR requires at least several

TABLE 2: Fitting Parameters for Two-photon Transient Absorption Data of All-trans Retinal in Hexane and Ethanol^a

λ probe (nm)	τ_1 (fs)	amp.	τ_2 (ps)	amp.	τ_3 (ps)	amp.
all-trans retinal in hexane						
450	190 ± 160	0.85			28 ± 6	-0.15
500	300 (fixed)	0.22	0.810	0.78		
550	300 (fixed)	0.75	1.2 ± 0.7	0.25	small	
600	180 ± 30	0.94			18	-0.06
all-trans retinal in ethanol						
500	300	0.81	1.8 (fixed)	0.19	small	
550	300 ± 230	0.72	1.8 (fixed)	0.28	small	
600	160 ± 100	0.69	1.8 (fixed)	0.06	35 ± 14	-0.25

^a Errors are based on a calculation of the standard deviation of a series of measurements. A "+" sign designates a decay in the absorption, and a "-" sign designates a rise in absorption. "Small" means that a slow component was discernible in the data, but its amplitude was too small to obtain a reliable time constant.

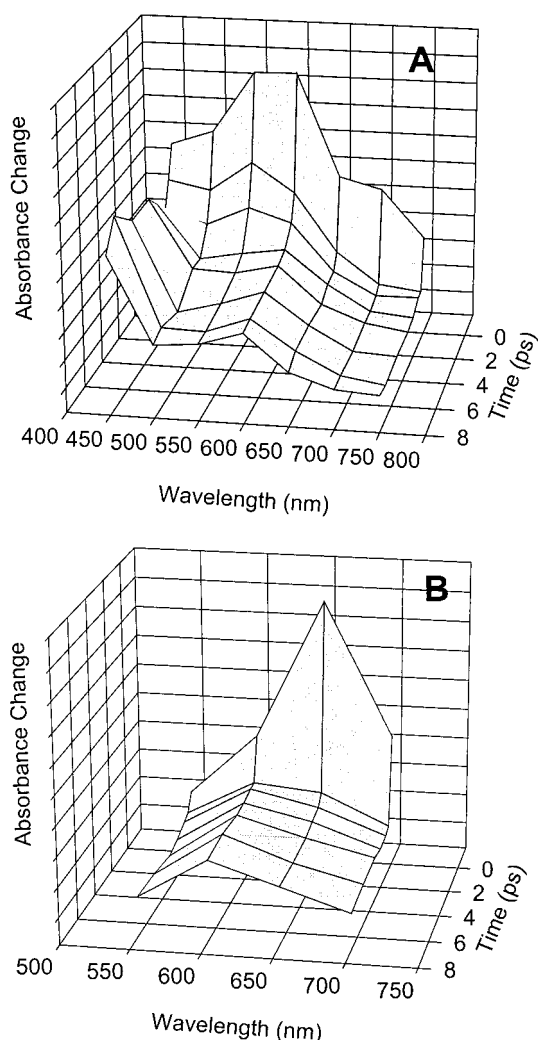


Figure 4. One- (A) and two-photon (B) induced transient absorption spectra of ATR in hexane. Spectra were constructed from single-wavelength measurements at 50-nm intervals. The vertical axis is the absorption change in units proportional to optical density. Excitation was at 400 (A) or 800 nm (B).

picoseconds to relax to the same state after excitation by OPE or TPE.

Figure 5 shows one- and two-photon induced transient absorption spectra of ATR in ethanol. In the one-photon induced spectra, an initial transient absorption peak at 550 nm decays

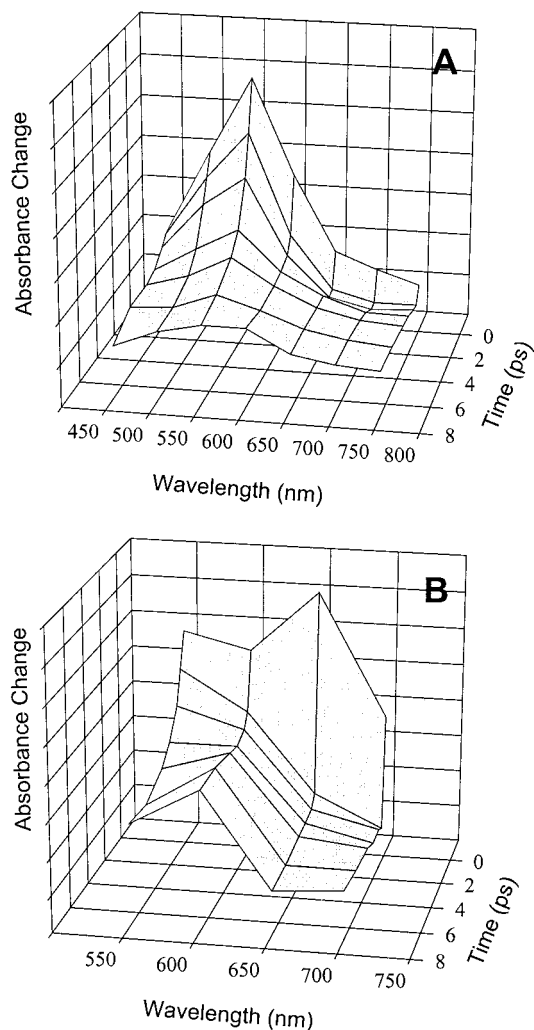


Figure 5. One- (A) and two-photon (B) induced transient absorption spectra of ATR in ethanol. Spectra were constructed from single-wavelength measurements at 50-nm intervals. The vertical axis is the absorption change in units proportional to optical density. Excitation was at 400 (A) or 800 nm (B).

smoothly over the first 8 ps. Stimulated emission gain appears at 650–750 nm and then decays over the same time regime. In contrast, the initial transient absorption in the two-photon induced transient absorption spectrum decays over the first 1–2 ps. A slower decay is observable at 550 nm. As for ATR in hexane, the one- and two-photon induced transient absorption spectra of ATR in ethanol are consistent with an increased weight of a subpicosecond decay component with two-photon excitation. Another important difference between the one- and two-photon induced transient absorption spectra is the presence of stimulated emission at 650–750 nm with one-photon excitation but not with two-photon excitation. These two features provide important clues for the assignment of relaxation events.

Analysis and Assignment of Relaxation. We seek a comprehensive interpretation of the one- and two-photon induced transient absorption results for ATR. Our analysis is based on the fact that OPE excites predominantly (but not exclusively) the "¹B_u⁺" state, whereas TPE preferentially excites the "¹A_g⁻" state,¹² so TPE induced transient absorption reveals relaxation events initiated in the "¹A_g⁻" state. However, in comparing one- and two-photon induced transient absorption responses, it is important to remember that OPE and TPE do not exclusively excite one state or the other. This is a consequence of the mixing of the "¹B_u⁺" and "¹A_g⁻" ππ* states,

which is expected to be enhanced by solvent polarity because the ${}^1\text{B}_u^+$ state, which has a higher oscillator strength, would be red-shifted more than the ${}^1\text{A}_g^-$ state.¹² Birge and co-workers have estimated the extent of mixing between ${}^1\text{B}_u^+$ and ${}^1\text{A}_g^-$ states and have compared the results to calculations.¹² The measurements were carried out for retinal in EPA (ethyl ether–isopentane–ethanol, 5:5:2) at 77 K. Birge and co-workers conclude that the extent of mixing between ${}^1\text{B}_u^+$ and ${}^1\text{A}_g^-$ states is at most 20%. They report an oscillator strength of 1.18 for the ${}^1\text{B}_u^+ \leftarrow \text{S}_0$ transition, compared to 0.125 for the ${}^1\text{A}_g^- \leftarrow \text{S}_0$ transition, a difference of nearly a factor of 10. For TPE, they report a measured a two-photon cross section for the ${}^1\text{A}_g^-$ state nearly 7 times larger than the two-photon cross section of the ${}^1\text{B}_u^+$ state. Thus, they conclude that the ${}^1\text{B}_u^+$ and ${}^1\text{A}_g^-$ states are legitimately characterized by the ${}^1\text{B}_u^+$ and ${}^1\text{A}_g^-$ states of linear polyenes, even in the polar EPA solvent.¹²

We consider first the ultrafast relaxation for ATR in ethanol. Similar considerations also apply to ATR in acetonitrile and propionitrile, where the response is similar (see below). The transient absorption is dominated by a 2-ps response at all wavelengths except 600 nm. This component can be assigned based on two observations. First, the 2-ps decay rate of stimulated emission in the 650–750 nm region associates the 2-ps component with a state having a large oscillator strength. As discussed above, this identifies the source of the stimulated emission with the ${}^1\text{B}_u^+$ state. We have argued previously that the 2-ps lifetime of the ${}^1\text{B}_u^+$ state is sufficient to account for the fluorescence quantum yield of retinal in ethanol and similar solvents.¹⁰ Because the radiative lifetime of the ${}^1\text{B}_u^+$ state was calculated from the absorption spectrum of ATR, it follows that the stimulated emission originates in the state that dominates the absorption band. This assignment is further supported by a comparison of the OPE and TPE induced transient absorption scans. In contrast to OPE induced transient absorption, where the 2-ps component dominates the response, in the TPE induced scans a faster component of 200–300 fs also appears. As noted above, TPE excites predominantly the ${}^1\text{A}_g^-$ state in contrast to OPE, which excites predominantly the ${}^1\text{B}_u^+$ state. The absence of stimulated emission upon TPE is further evidence that the stimulated emission originates in the ${}^1\text{B}_u^+$ state. Thus, the comparison of OPE and TPE induced spectra supports the assignment of the 2-ps component to the decay of the ${}^1\text{B}_u^+$ state. The appearance of a 200–300 fs component in TPE induced transients further suggests that this component be assigned to the decay of the ${}^1\text{A}_g^-$ state. These results support the assignments made previously.⁶

An interesting feature of the OPE induced transient response of ATR in ethanol is the fast appearance of stimulated emission gain at 700 and 750 nm. The emission is shifted to the red from an absorption band around 400–450 nm. The time scale of this response appears to be <200 fs, a value that is faster than the initial solvation response of 290 fs that has been reported for ethanol.¹⁷ This finding suggests that the most important contribution to the Stokes shift arises from intramolecular relaxation rather than from the solvation response of the solvent. The large red-shift of the peak fluorescence wavelength relative to the absorption band indicates a structural change in the excited ${}^1\text{B}_u^+$ state. Displacement of the excited-state potential surface, which is expected to occur along C=C stretching modes,¹⁸ would contribute a very fast intramolecular Stokes shift that is not resolvable in the present experiments.

We consider next the ultrafast photophysics for ATR in hexane. The response differs in several respects from the

photophysics of ATR in ethanol. In contrast to the response of ATR in ethanol, no stimulated emission is detectable for ATR in hexane. Furthermore, the OPE induced response in hexane contains a 200–300 fs component as well as a \sim 2-ps component, whereas the response of ATR in ethanol contains only a 2-ps component over the first 10 ps. On a longer time scale, transient absorption grows in at 450 nm with a time constant of 29 ± 6 ps. The appearance time for this absorption corresponds to ISC, and this component can be attributed to $\text{T}_n \leftarrow \text{T}_1$ absorption.¹

Two-photon induced transient absorption signals were also obtained for ATR in hexane. A comparison of the OPE and TPE induced transient absorption scans for ATR in hexane shows that the 200–300 fs component is more dominant with TPE. The 2-ps component, which was detected with amplitudes of 10–20% in OPE induced transient absorption at 450–650 nm, could only be detected at 500 and 550 nm in TPE induced transient absorption scans (Figure 3). Similarly to ATR in ethanol, the stronger weighting of the fast (200–300 fs) response by TPE can be associated with relaxation of the ${}^1\text{A}_g^-$ state for ATR in hexane. However, we must also account for the presence of a \sim 300-fs component for OPE of ATR in hexane. Clearly this component would not be detected in the sequential decay ${}^1\text{B}_u^+ \rightarrow {}^1\text{A}_g^- \rightarrow n\pi^*$, since the slower 2-ps decay of the ${}^1\text{B}_u^+$ state would render the faster decay component undetectable. Thus we have argued previously⁶ that this component results at least in part from initial excitation of the ${}^1\text{A}_g^-$ state by OPE at 400 nm via its weak but nonnegligible oscillator strength ($f \approx 0.07$ ¹²).

One factor in the difference between the relative contributions of the ${}^1\text{B}_u^+$ and ${}^1\text{A}_g^-$ states to transient spectra of ATR in hexane and ethanol arises simply from solvent-induced shifts in the ground-state absorption spectra. Since both the ${}^1\text{B}_u^+$ and ${}^1\text{A}_g^-$ states possess dipole moments,¹² these bathochromic shifts result from solvation by a polar solute. For ATR in ethanol, the peak of the one-photon absorption spectrum is at 385 nm. The peak of the two-photon excitation is expected to be 2400 cm^{-1} to lower energy, based on a comparison of one- and two-photon spectra for ATR in the polar solvent EPA.¹² In contrast, for ATR in a nonpolar solvent such as hexane, the one-photon absorption spectrum is blue-shifted to 365 nm. It seems reasonable to expect that the TPE spectrum is also blue-shifted. Thus for OPE at 400 nm or TPE at 800 nm, we anticipate a stronger overlap with the ${}^1\text{B}_u^+$ state for ATR in polar solvents than in nonpolar solvents, and, conversely, a stronger overlap with the ${}^1\text{A}_g^-$ state in nonpolar solvents than in polar solvents. These trends are consistent with a stronger relative contribution from the subpicosecond relaxation assigned to the ${}^1\text{A}_g^-$ state in hexane than in ethanol by one-photon excitation. Therefore, it is possible to attribute the two components (≤ 300 fs and ~ 2 ps) to parallel relaxation of ${}^1\text{B}_u^+$ and ${}^1\text{A}_g^-$ states.

However, the above explanation alone fails to explain why the fluorescence quantum yield of ATR in hexane is much smaller than that for ATR in ethanol, since, as described above, a 2-ps lifetime of the ${}^1\text{B}_u^+$ state is associated with a quantum yield of $\sim 2 \times 10^{-4}$, irrespective of solvent. Another possibility is that a subpopulation of ATR that relaxes in ≤ 300 fs may exist in hexane. The existence of distinct subpopulations of retinal with different decay times of the ${}^1\text{B}_u^+$ state was demonstrated for ATR in an alkane solvent (3-methylpentane) and in ethanol at low temperatures,¹⁰ and these populations may persist at room temperature, with one population where the ${}^1\text{B}_u^+$ relaxes in ca. 2 ps and another where an additional,

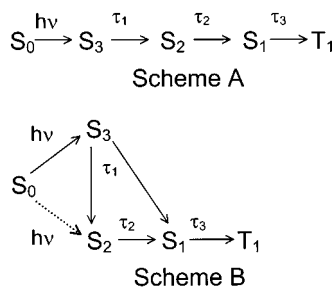


Figure 6. Kinetic models for ultrafast relaxation of all-trans retinal. Scheme A assumes sequential relaxation with $\tau_1 < \tau_2 < \tau_3$. In Scheme B, states S_3 and S_2 can be excited simultaneously and relax in parallel. S_3 is excited preferentially by one-photon excitation, whereas S_2 is excited preferentially to two-photon excitation. In B, $\tau_1 = 2$ ps and $\tau_2 \approx 300$ fs. S_3 may relax by internal conversion to S_2 or directly to S_1 . In polar solvents, a subpopulation of ATR is favored where $\tau_1 = 2$ ps and $\tau_2 \approx 300$ fs. In nonpolar solvents, a second population is favored with faster relaxation from S_3 . Relaxation back to S_0 , for example by internal conversion from S_1 or decay of T_1 , has been left out for simplicity.

faster, channel of relaxation of the “ $^1B_u^+$ ” state opens up. The fraction of retinal in each of the populations appears to be sensitive to solvent polarity. A subpopulation of ATR in hexane with a faster decay of the “ $^1B_u^+$ ” state would explain the lower fluorescence quantum yield of ATR in hexane compared to more polar solvents. Because the fluorescence quantum yield of ATR in ethanol can be accounted for by emission from the “ $^1B_u^+$ ” state, a shorter “ $^1B_u^+$ ” lifetime in a subpopulation of ATR would lead to a decreased fluorescence quantum yield. The decay time for this fast relaxation is not resolved in our measurements from the subpicosecond component associated with decay of the “ $^1A_g^-$ ” state.

Models of Retinal Photophysics. Two possible kinetic models for the assignment of relaxation processes in ATR are depicted in Figure 6. One view^{7,8,11} (Figure 6A) assumes that the observed kinetics follow sequential relaxation in successively slower steps from S_3 (“ $^1B_u^+$ ”) \rightarrow S_2 (“ $^1A_g^-$ ”) \rightarrow S_1 ($n\pi^*$). A rise time associated with formation of the S_2 (“ $^1A_g^-$ ”) state has not been identified,^{6,8} suggesting either that the S_3 (“ $^1B_u^+$ ”) \rightarrow S_2 (“ $^1A_g^-$ ”) step is extremely fast and unresolved (as proposed by Yamaguchi and Hamaguchi⁸) or that the sequential kinetic scheme is incorrect. Within kinetic model A, Yamaguchi and Hamaguchi assigned lifetimes of 30 fs to the “ $^1B_u^+$ ” state, 0.72 ps to the “ $^1A_g^-$ ” state, and 32 ps to the $n\pi^*$ state for ATR in hexane.⁸ For ATR in 1-butanol,¹¹ a lifetime of 200 fs was assigned to the “ $^1B_u^+$ ” state, a lifetime of 1.6 ps to the “ $^1A_g^-$ ” state, and a lifetime of 22 ps to the $n\pi^*$ state.¹¹ These assignments encounter two principal difficulties. First, the detection of stimulated emission with a decay time of ~ 2 ps, both for ATR in ethanol⁶ and for ATR in 1-butanol¹¹ shows that the emitting state has a large oscillator strength. Yamaguchi and Hamaguchi assumed that the oscillator strength of the “ $^1A_g^-$ ” $\leftarrow S_0$ transition is at least as strong as that of the “ $^1B_u^+$ ” $\leftarrow S_0$ transition,¹¹ in contradiction to the measurements of Birge and co-workers.¹² Second, kinetic model A does not account for the two-photon induced transient absorption spectra, where the relative contribution of the fast (200–300 fs) response increases and the relative contribution of the 2-ps response decreases compared to those of the one-photon induced transient absorption spectra.

We have proposed another model (Figure 6B) based on a comparison of the OPE and TPE induced transients.⁶ In this model, we assign the ~ 2 -ps response to relaxation from the S_3 (“ $^1B_u^+$ ”) state and the 200–300 fs lifetime to the “ $^1A_g^-$ ” state.

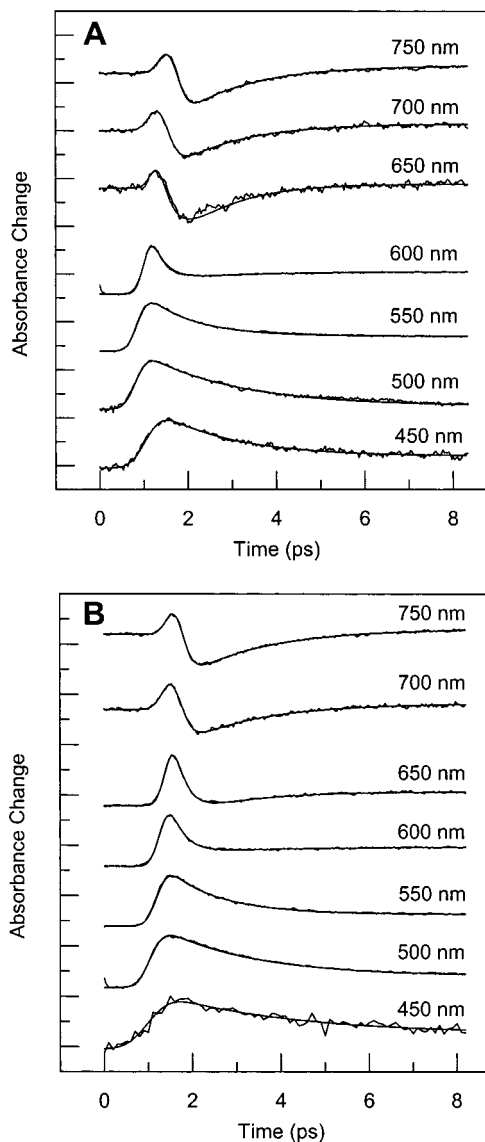


Figure 7. One-photon induced transient absorption scans of ATR in (A) acetonitrile and (B) propionitrile. Excitation was at 400 nm. The smooth solid lines show fits to the data. Scans have been normalized.

The increased weight of this fast component in TPE relative to OPE-induced transient absorption can be understood as a result of the 7-fold higher two-photon cross section of the “ $^1A_g^-$ ” state relative to the “ $^1B_u^+$ ” state. We think that model B is well supported for ATR in ethanol because, in addition to the evidence from the comparison of OPE and TPE, the 2-ps component in the decay of stimulated emission identifies the 2-ps component with a state having a strong oscillator strength, namely the “ $^1B_u^+$ ” state. The comparison of OPE and TPE induced transient absorption (see Figures 2 and 3) suggests that this scheme applies to ATR in the nonpolar solvent hexane as well. Furthermore, as described above, indirect evidence (the lower fluorescence yield for ATR in hexane and low-temperature measurements¹⁰) suggests the existence of a subpopulation of ATR in hexane where the lifetime in the emissive “ $^1B_u^+$ ” state is short ($\lesssim 300$ fs). In this subpopulation, a faster relaxation channel leads to relaxation of the “ $^1B_u^+$ ” state in less than 300 fs, resulting in the lower fluorescence quantum yield of ATR in nonpolar solvents. This suggests that the decay of the S_3 state is sensitive to the conformation of ATR. Nonpolar solvents may favor a conformation where a fast decay channel is open for S_3 , which is closed in the conformation favored in polar

TABLE 3: Fitting Parameters for One-Photon Transient Absorption Data of All-trans Retinal in Acetonitrile and Propionitrile^a

λ probe (nm)	τ_1 (fs)	amp.	τ_2 (ps)	amp.	τ_3 (ps)	amp.
all-trans retinal in acetonitrile						
450			1.7	0.80	19 ± 3	0.20
500			2.2 ± 0.3	0.84	33 ± 6	0.16
550			0.86 ± 0.3	0.92	37	0.08
600	300 (fixed)	0.83	1.2 ± 0.4	-0.17		
650	300 (fixed)	0.63	1.0 ± 0.3	-0.32	15 ± 1	0.05
700	300 (fixed)	0.67	1.2	-0.33		
750	300 (fixed)	0.79	1.2	-0.36		
all-trans retinal in propionitrile						
450			3.0	0.94	48	0.06
500			2.0 ± 0.1	0.94	48	0.06
550	300 (fixed)	0.14	1.2 ± 0.1	0.75	17 ± 8	0.11
600	300 (fixed)	0.86	2.6 ± 1.9	-0.14		
650	250 ± 20	0.81	1.3 ± 0.2	-0.15	14 ± 1	0.04
700	200 ± 100	0.77	1.6 ± 0.2	-0.21	40	0.02
750	160 ± 60	0.77	1.6 ± 0.4	-0.23		

^a Errors are based on a calculation of the standard deviation of a series of measurements.

solvents. The S_3 decay rate in the slow-decaying subpopulation is strongly temperature dependent.¹⁰

Retinal Photophysics in Polar Aprotic Solvents. The results described in the preceding sections compare electronic relaxation of ATR in the protic solvent ethanol and the nonpolar solvent hexane. However, the nature of the interaction with protic solvents remains unclear. The effect of protic solvents may result from solvent polarity, or, alternatively, protic solvents could act specifically through hydrogen-bond formation. To determine whether specific effects of hydrogen bonding arise in protic solvents, we here compare the transient absorption response of ATR in the nonprotic, polar solvents acetonitrile and propionitrile with the response in the protic solvent ethanol. The results are shown in Figure 7 with decay times in Table 3. It is readily apparent that the transient absorption of ATR in the nitriles is highly similar to that in ethanol. As in ethanol, a \sim 2-ps transient is observed at all probe wavelengths. This component appears as a transient absorption decay for probe wavelengths of 450–550 nm and as a decay of stimulated emission gain for probe wavelengths of 600–750 nm. In fact, the transient absorption responses in ethanol and acetonitrile are nearly indistinguishable. As for ATR in ethanol, the 2-ps stimulated emission response can be assigned to emission from S_3 (${}^4B_u^+$). In propionitrile, a similar response is observed. However, stimulated emission is observed only at 700 and 750 nm, and not at 650 nm, as it is in the more polar solvents ethanol and acetonitrile. ISC for retinal in nitriles also appears to be similar to that in ethanol. As in ethanol, the rise time of the triplet–triplet absorption is about 28 ps (data not shown). The amplitude of the triplet–triplet absorption rise at 450 nm is very small, consistent with the low ISC quantum yield that has been reported for ATR in acetonitrile.¹³ (The triplet yield of ATR in acetonitrile is 0.1, comparable to the triplet yield of ATR in ethanol of 0.08–0.13¹³).

The similarity of the transient absorption in ethanol and nitriles suggests that the assignment of excited-state relaxation processes is similar in these solvents. Correspondingly, this finding suggests that the nature of the excited states is very likely to be similar in the polar aprotic and protic solvents. Therefore, we conclude that solvent polarity can account for the response of ATR in ethanol. Thus, although H-bonded complexes of ATR form,^{19,20} the effect of hydrogen-bonding on the excited-state dynamics seems to be indistinguishable from

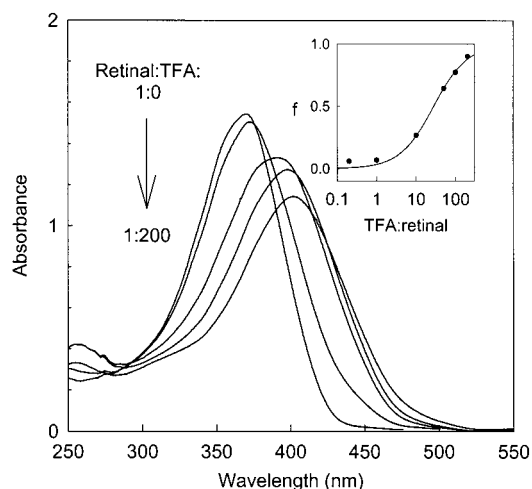


Figure 8. Steady-state absorption spectra of ATR in hexane with TFA added at retinal:TFA ratios of 1:0, 1:10, 1:50, 1:100, and 1:200. The retinal concentration was 3.5×10^{-4} M. The inset shows the fraction of hydrogen-bonded retinal estimated from the absorbance at 450 nm (see text). The solid line in the inset shows the fraction of hydrogen-bonded retinal for a hydrogen-bonding association constant of 104 M^{-1} .

the effect of solvent polarity, suggesting that, at least for moderate H bond donors, there is not a unique effect of hydrogen bonding apart from the effect of polarity.

Analysis of Hydrogen-Bonding Effects. Further experiments were carried out to investigate the specific effects of hydrogen bonding by measuring transient absorption spectra of ATR in mixed solvents containing hydrogen-bond donors. Trifluoroacetic acid (TFA), a strong hydrogen-bond donor, was introduced into solutions of ATR in hexane. Ground-state absorption spectra are shown in Figure 8 for all-trans retinal in hexane with TFA added as a cosolvent. As the ratio of TFA to ATR is increased, a red-shifted species is observed, first as a shoulder on the long-wavelength side of the absorption band and then as the main absorption band at higher TFA/ATR concentrations. We attribute this feature to hydrogen-bonded ATR.¹⁹ The absence of an isosbestic point shows that the spectrum of one or both components is shifting with increasing TFA concentration. This may result from an increasing polarity of the solution that causes red-shifts in the spectra. Nevertheless, we can estimate the equilibrium constant for hydrogen bond formation:



for which

$$K_{\text{eq}} = \frac{f}{(1-f)(r-f)[\text{ATR}]_{\text{tot}}} \quad (3)$$

where f is the fraction of ATR in the hydrogen bonded form and r is the ratio of total TFA to total ATR concentrations. The fraction f of hydrogen-bonded retinal was estimated from the absorbance of ATR-TFA at 450 nm, where the absorbance of non-hydrogen-bonded retinal is negligible. (The absorption coefficient of hydrogen-bonded retinal at 450 nm was obtained from a Benesi–Hildebrandt plot²¹ incorporating only points for TFA/ATR ratios of 10 or larger for which the TFA concentration could be approximated by the initial TFA concentration as required by the Benesi–Hildebrandt method.) The inset in Figure 8 shows a plot of the fraction f of ATR-TFA with $K_{\text{eq}} = 104$.

Transient absorption scans of ATR in hexane with retinal to TFA ratios ranging from 5:1 to 1:200 are shown in Figure 9.

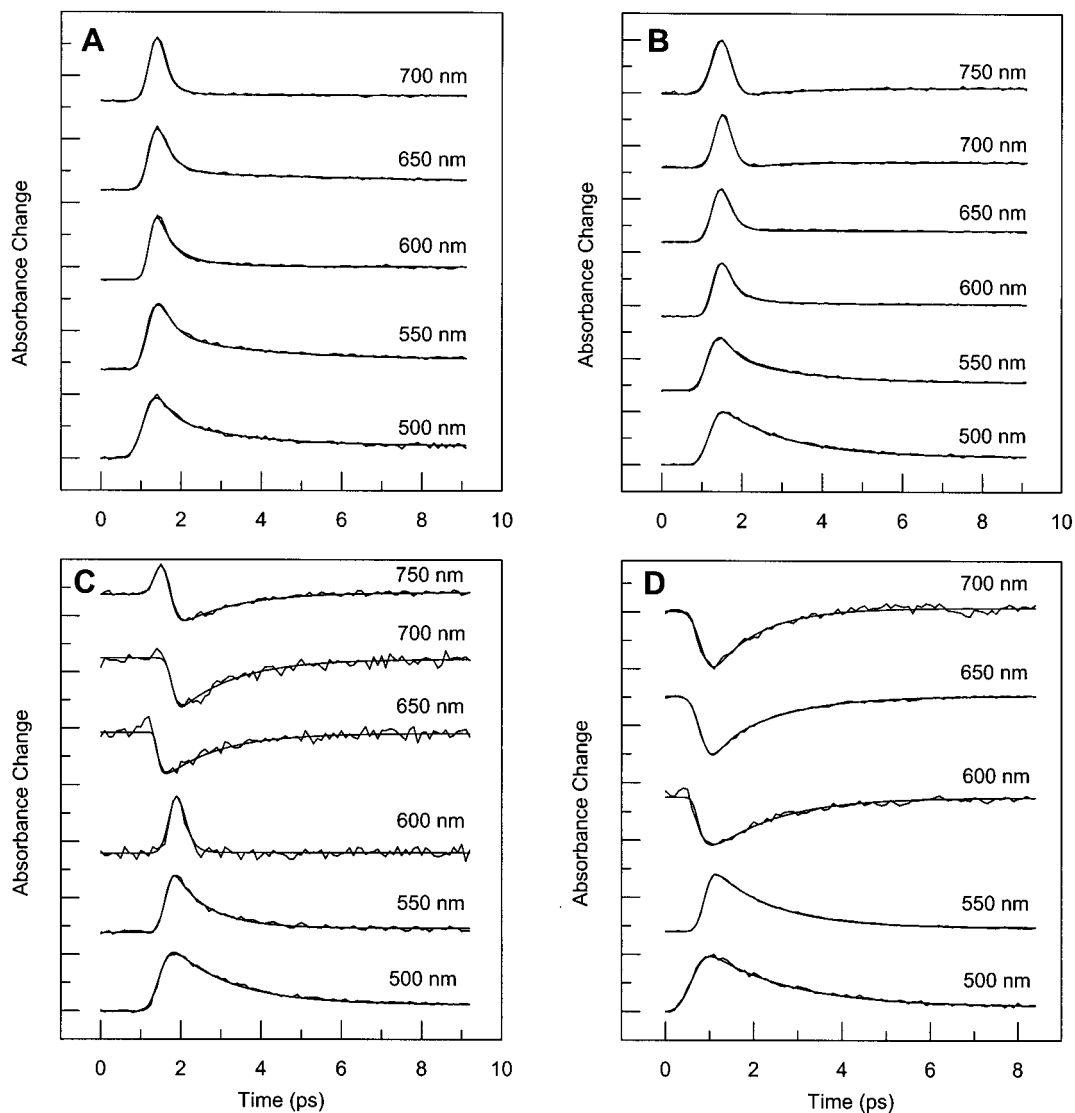


Figure 9. One-photon induced transient absorption scans of ATR in hexane and TFA. The molar ratio of retinal to TFA is (A) 5:1, (B) 1:1; (C) 1:10, and (D) 1:200. Excitation was at 400 nm. The smooth solid lines show fit to the data. Scans have been normalized.

Fitting parameters are tabulated in Table 4. Several observations can be made from these results. The transient response for a retinal/TFA ratio of 5:1 is essentially identical to the response of retinal in pure hexane (compare Figure 2). With increased concentration of TFA, the nature of the transient response changes smoothly from resembling the response of ATR in hexane at a ratio of 5:1 to resembling the response of ATR in ethanol for a ratio of 1:10, where about 30% of ATR is hydrogen-bonded. A change in the ratio of retinal/TFA from 1:1 to 1:10 is sufficient to shift the response at long wavelengths from excited-state absorption (as observed in hexane) to stimulated emission (as observed in ethanol).

As the ratio of the TFA cosolvent increases, an increasingly strong contribution with a time constant of ~ 2 ps is detected. Concurrently, stimulated emission gain is observed, first very weakly at 750 nm for a 1:1 retinal/TFA ratio, then in the 650–750 nm region for a 1:10 retinal/TFA ratio, and finally from 600 to 750 nm for a ratio of 1:200, where almost all ATR is hydrogen-bonded. Thus, for a low concentration of hydrogen-bond donor, stimulated emission gain is observed only at longer wavelengths. Then, as the hydrogen-bond donor concentration increases, stimulated emission becomes increasingly strong, and the wavelengths at which it is observable expand toward the blue. The fluorescence spectrum of ATR has been reported in

the presence of the hydrogen-bond donors trifluoroacetic acid¹⁹ and hexafluoro-2-propanol.²² In both cases, a broad emission spectrum was observed peaking at 500–550 nm with a tail extending toward 600–700 nm. The fact that stimulated emission is observed only in the 650–750 nm region suggests the existence of excited-state absorption in the 500–700 nm region that competes with stimulated emission. At weak concentrations of hydrogen-bond donor (retinal/TFA ratios of 5:1 and 1:1; see parts A and B of Figure 9), the excited-state absorption dominates, and stimulated emission is observed, if at all, at 700–750 nm. For an ATR/TFA ratio of 1:10, the excited-state absorption and stimulated emission nearly cancel each other out at 600 nm, where an underlying faster response can be detected. For an ATR/TFA ratio of 1:200, the stimulated emission is stronger, and in fact for an ATR/TFA ratio of 1:200, the stimulated emission gain is stronger than that observed in ethanol.

The increased stimulated emission observed with increasing concentration of hydrogen-bond donor is consistent with the increase in fluorescence quantum yield that was observed when TFA was added to solutions of retinal in hexane or methanol¹⁹ or when hexafluoro-2-propanol was added to solutions of retinal in cyclohexane.²² The increased stimulated-emission component may arise from a shift in the partitioning of ATR into

TABLE 4: Fitting Parameters for One-Photon Transient Absorption Data of All-trans Retinal in Hexane with Trifluoroacetic Acid (TFA)^a

λ probe (nm)	τ_1 (fs)	amp.	τ_2 (ps)	amp.	τ_3 (ps)	amp.
5:1 retinal/TFA molar ratio						
500	300 (fixed)	0.67	1.9	0.33	small	–
550	300 (fixed)	0.76	2.3	0.24	small	+
600	300 (fixed)	0.66	0.78	0.29	29	0.05
650	320	1.0			small	+
700	330	1.0			small	+
750					32	1.0
1:1 retinal/TFA molar ratio						
500			1.6	1.0	small	–
550	300 (fixed)	0.62	1.9	0.33	20	0.05
600	250	0.86	0.79	0.10	21	0.04
650	220	0.84			14	0.16
700	170	0.88	0.62	–0.11	18	0.01
750			1.4	–0.92	28	0.08
1:10 retinal/TFA molar ratio						
500			1.5	1.0	small	+
550			1.2 ± 0.2	0.67	33	0.33
600					38	1.0
650			1.3 ± 0.2	–0.58	30	0.42
700			1.2 ± 0.2	–0.92	48	0.08
750			1.3 ± 0.1	–1.0	small	+
1:200 retinal/TFA molar ratio						
500			1.9	1.0		
550			1.2 ± 0.2	1.0	small	+
600			1.7 ± 0.4	–1.0	small	+
650			1.5	–1.0	small	+
700			1.1	–1.0	small	+

^a Amplitude columns show relative amplitudes of the decay components. A positive amplitude designates a decay in the absorption, whereas a negative amplitude designates a rise. “Small” indicates that the amplitude of a particular decay was too small to obtain an accurate rate constant.

subpopulations, as discussed above. The increased fluorescence yield in polar solvents and in the presence of hydrogen-bond donors then results from an increasing fraction of ATR in the population that relaxes slowly (~ 2 ps at room temperature) out of the “ $^1B_u^+$ ” state.

Conclusions

We have described ultrafast transient absorption measurements of all-trans retinal excited by one- and two-photon transitions. Because OPE and TPE launch the excited-state photophysics in different initial states, a comparison of OPE and TPE induced transient absorption leads to the following assignment of lifetimes of the three excited singlet states for ATR in hydrogen-bonded and polar solvents: S_3 “ $^1B_u^+$ ” (2 ps), S_2 “ $^1A_g^-$ ” (200–300 fs), and S_1 $^1n\pi^*$ (20–30 ps). The proposed model accounts for the dependence of relaxation on solvent and on mode of excitation (OPE or TPE). The decay of S_3 is observed by OPE, whereas the decays of both S_2 and S_3 in parallel are observed by TPE. We have shown previously that the 2-ps decay of the “ $^1B_u^+$ ” state accounts for the observed fluorescence yield of ATR in ethanol.¹⁰ The response in the polar protic solvent ethanol and in the polar nonprotic solvents acetonitrile and propionitrile are similar, including stimulated emission at probe wavelengths of 650–750 nm, suggesting that the solvent influences the excited-state relaxation primarily through solvent polarity. In contrast, no stimulated emission was

detected in the nonpolar solvent hexane, consistent with the lower fluorescence yield in dry hydrocarbon solvents. The role of hydrogen bonding was investigated by addition of a hydrogen-bond donor, trifluoroacetic acid, to ATR in hexane. With increasing concentration of TFA, the transient absorption changed smoothly from one characteristic of a nonpolar solvent to one characteristic of a polar solvent. We detected no evidence for new excited-state processes involving proton transfer or excited-state hydrogen-bond formation or dissociation. This suggests that hydrogen bonds act mainly through the introduction of a more polar local environment. The results are consistent with the previous finding¹⁰ that all-trans retinal exists in (at least) two populations with different “ $^1B_u^+$ ”-state lifetimes. Polarity favors a population of retinal characterized by stimulated emission from the “ $^1B_u^+$ ” state and a low triplet yield. In contrast, in nonpolar solvents, a larger subpopulation is present with faster decay of the “ $^1B_u^+$ ” state, resulting in a lower fluorescence quantum yield.

Acknowledgment. We thank Prof. H. Hamaguchi for communicating a preprint¹¹ prior to publication. This work was supported in part by NSF EPSCoR Grant No. 9550487. E.J.L. acknowledges support by a Training Grant in Chemical Biology (NIH GM08545).

Note Added after ASAP Posting. This article was released ASAP on 08/14/2001 with an error in the expression $^1A_g^-$. The correct version was posted on 08/21/2001.

References and Notes

- (1) Hochstrasser, R. M.; Narva, D. L.; Nelson, A. C. *Chem. Phys. Lett.* **1976**, *43*, 15–19.
- (2) Birge, R. R. *Annu. Rev. Biophys. Bioeng.* **1981**, *10*, 315–354.
- (3) Becker, R. S. *Photochem. Photobiol.* **1988**, *48*, 369–399.
- (4) Tahara, T.; Hamaguchi, H. *Chem. Phys. Lett.* **1995**, *234*, 275–280.
- (5) Yamaguchi, S.; Hamaguchi, H. *J. Mol. Struct.* **1996**, *379*, 87–92.
- (6) Larson, E. J.; Friesen, L. A.; Johnson, C. K. *Chem. Phys. Lett.* **1997**, *265*, 161–168.
- (7) Takeuchi, S.; Tahara, T. *J. Phys. Chem. A* **1997**, *101*, 3052–3060.
- (8) Yamaguchi, S.; Hamaguchi, H. *J. Chem. Phys.* **1998**, *109*, 1397–1408.
- (9) Yamaguchi, S.; Hamaguchi, H. *Chem. Phys. Lett.* **1998**, *287*, 694–700.
- (10) Larson, E. J.; Johnson, C. K. *J. Phys. Chem. B* **1999**, *103*, 10917–10923.
- (11) Yamaguchi, S.; Hamaguchi, H. *J. Phys. Chem. A* **2000**, *104*, 4272–4279.
- (12) Birge, R. R.; Bennett, J. A.; Hubbard, L. M.; Fang, H. L.; Pierce, B. M.; Klinger, D. S.; Leroy, G. E. *J. Am. Chem. Soc.* **1982**, *104*, 2519–2525.
- (13) Das, P. K.; Becker, R. S. *J. Am. Chem. Soc.* **1978**, *101*, 6348–6353.
- (14) Takemura, T. K.; Das, P. K.; Hug, G.; Becker, R. S. *J. Am. Chem. Soc.* **1976**, *98*, 7099–7101.
- (15) Takemura, T. K.; Das, P. K.; Hug, G.; Becker, R. S. *J. Am. Chem. Soc.* **1978**, *100*, 2626–2630.
- (16) English, D. S.; Zhang, W.; Kraus, G. A.; Petrich, J. W. *J. Am. Chem. Soc.* **1997**, *119*, 2980–2986.
- (17) Horng, M. L.; Gardecki, J. A.; Papazyan, A.; Maroncelli, M. *J. Phys. Chem.* **1995**, *99*, 17311–17337.
- (18) Garavelli, M.; Vreven, T.; Celani, P.; Bernardi, F.; Robb, M. A.; Olivucci, M. *J. Am. Chem. Soc.* **1998**, *120*, 1285–1288.
- (19) Alex, S.; Thanh, H. L.; Vocelle, D. *Can. J. Chem.* **1992**, *70*, 880–887.
- (20) Dawson, W.; Abrahamson, E. W. *J. Phys. Chem.* **1962**, *66*, 2542–2547.
- (21) Benesi, H. A.; Hildebrand, J. H. *J. Am. Chem. Soc.* **1949**, *71*, 2703–2707.
- (22) Das, P. K.; Hug, G. L. *Photochem. Photobiol.* **1982**, *36*, 455–461.